

# The Dark Side of CIELAB

Gaurav Sharma and Carlos Eduardo Rodríguez-Pardo  
ECE Dept. Univ. of Rochester, Rochester, NY, USA

## ABSTRACT

Standardized in 1976 as a uniform color space, CIELAB is extensively utilized in color science and engineering applications. CIELAB provides both a color difference formula and correlates for common perceptual descriptors of color. Deficiencies in both areas are well-known, and based on these known limitations, numerous fixes have been developed yielding alternative color difference formulae that are derived as modifications of the color difference in CIELAB. In addition, several new color appearance spaces have also been proposed as modifications of the basic CIELAB framework.

In this paper, we point out other, lesser-known and poorly-appreciated, limitations of CIELAB that occur particularly in the dark regions of color space. We demonstrate via examples, how these limitations not only cause performance compromises but lead to fundamental breakdowns in system optimization and design problems, making CIELAB unusable in these problems. We consider the reasons why these fundamental limitations were overlooked in the original development of CIELAB and analyze the mathematical representations contributing to the undesired behavior. We argue that fundamental new research is required to overcome this dark side of CIELAB; the development of uniform color spaces and new color appearance spaces must be revisited afresh using new experimental data and keeping in mind newer devices and applications.

**Keywords:** CIELAB, Uniform Color Spaces, Display Color Optimization

## 1. INTRODUCTION

Consider a simple visual experiment, where a stimulus of the format shown in Fig. 1 is presented to an observer. The observer is asked to compare the two patches placed on a white background, one of which is an ideal black, emitting no light whatsoever, and the other represents a monochromatic spectrum, such as one that would be obtained by spatially diffusing a laser beam. Now suppose that we decrease the intensity of the monochromatic patch. Our intuition and experience suggest that in this setting, as the monochromatic patch gets darker approaching a match with the black patch, its chroma also decreases; in the immediate vicinity of black, the chroma is also necessarily small. When we attempt to numerically compute correlates of color perception for this experimental setting using the CIELAB color space\*, however, we encounter a rather surprising and large anomaly that is illustrated in Fig. 2.

Sub-figures 2(a), 2(b), and 2(c), represent traces in the  $a^* - b^*$  plane for monochromatic stimuli spanning the visible spectral range from 400 to 700 nm, where the  $L^*$  value is maintained constant for the points presented within each sub-figure, the three sub-figures corresponding to  $L^*$  values of 0.5, 0.25, and 0.1, respectively. As can be seen from these figures, the CIELAB predictions are in very significant disagreement with our experience, particularly for the dark monochromatic spectra in the short wavelength region from 400 to 460 nm. Even at these rather low  $L^*$  values (recall, that  $L^* = 100$  represents the adaptation white and  $L^* = 0$  represents the ideal black), the monochromatic spectra in these color regions exhibit extremely large chroma values. We believe that these CIELAB predictions represent relatively large deviations from actual perception and represent a dark side of the CIELAB color space representation, which plagues it particularly in the dark regions of color, make the title of our paper a double entendre.

---

Further author information:

G.S.: E-mail: gaurav.sharma@rochester.edu, Telephone: 1 585 275 7313

C.R.: E-mail: pardo@ece.rochester.edu, Telephone: 1 585 275 8122

C.E. Rodriguez-Pardo is supported in part by a grant from Sharp Labs America.

\*A formal summary of CIELAB will be provided subsequently in Section 2 after this motivating example.

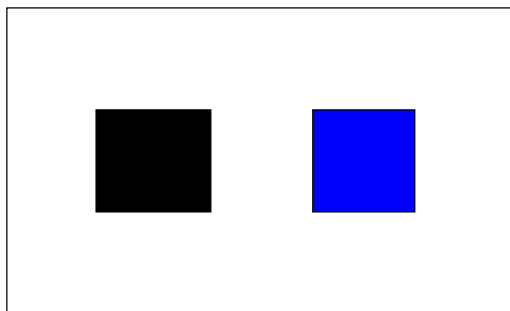


Figure 1. Hypothetical visual experiment: Comparing two patches against a white background.

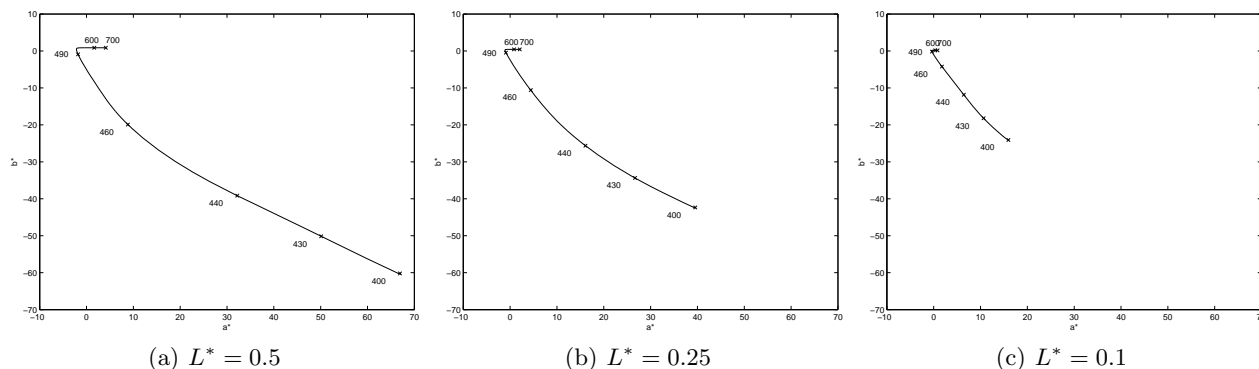


Figure 2. Paths traced by constant  $L^*$  monochromatic stimuli in the  $a^* - b^*$  plane. Sub-figures 2(a), 2(b), and 2(c) correspond to  $L^*$  values of 0.5, 0.25, and 0.1, respectively.

Our primary objectives in presenting this paper are to highlight the challenge that this dark side of CIELAB poses in color imaging applications and to stir further debate within the community. To initiate this debate, we speculate on the origins of the specific problem and on potential alternative approaches for developing uniform color spaces with appearance correlates that may well resolve these challenges while maintaining mathematically and computationally desirable attributes of CIELAB. Fresh effort is needed in this area of color science research.

The rest of this paper is organized as follows. Section 2 provides a short background on the CIE system and the CIELAB color space, with a view to facilitating the follow on discussion and making the paper accessible to individuals not already familiar with CIELAB. In Section 2 we revisit the dark side of CIELAB outlining the challenges it poses for imaging applications using a case study from display gamut optimization where the problems prove to be particularly pernicious. Section 4 presents a discussion including a speculation on the underlying causes for the limitations of CIELAB in the dark regions and on simple techniques that can be used to analyze the mathematical behavior of proposed color space transformations. Section 5 provides a concluding summary.

## 2. CIELAB BACKGROUND

The CIE system for colorimetry<sup>1</sup> provides a framework for specification of color sensations. Within the CIE system, colors can be specified in terms of their X, Y, and Z tristimulus values, which, for a light stimulus with power spectral density  $f(\lambda)$ , are given by<sup>1</sup>

$$\begin{aligned}
 X &= \int \bar{x}(\lambda)f(\lambda)d\lambda \\
 Y &= \int \bar{y}(\lambda)f(\lambda)d\lambda \\
 Z &= \int \bar{z}(\lambda)f(\lambda)d\lambda
 \end{aligned} \tag{1}$$

where  $\bar{x}(\lambda)$ ,  $\bar{y}(\lambda)$ , and  $\bar{z}(\lambda)$  are the CIEXYZ color matching functions. The tristimulus values have the property that under identical viewing conditions stimuli with identical CIEXYZ tristimuli match for the “CIE normal observer” which is representative of color normal viewers. The CIEXYZ tristimulus system provides a numerical specification of color and represents a very significant advance, particularly in view of the fact that, among our five senses, hearing is the only other sense for which numerical specification is feasible and for the three senses of taste, touch, and smell, to this day, no robust system exists for the numerical specification of sensations.<sup>2-4</sup>

For practical use in color imaging applications, additional properties, beyond the matching characterization provided by the CIEXYZ tristimulus values, are desirable for a system for numerical specification of color. Two such properties include *perceptual uniformity* and the availability of *correlates for perceptual attributes* of color. Perceptual uniformity refers to the property that equal (Euclidean) distances in the color space representation correspond to equal perceived differences [5, Chap. 6], a trait that has clear and direct relevance in establishing tolerances for color reproduction. Because no considerations of perceptual uniformity played a role in the selection of the CIEXYZ tristimulus specification, the CIEXYZ space is perceptually nonuniform and therefore not well suited to the specification of color tolerances for color imaging applications. Similarly, the coordinates in CIEXYZ space do not directly provide correlates for the common perceptual attributes such as *hue*, *lightness*, and *chroma*<sup>†</sup>. In order to allow representation and manipulation of colors in an intuitive manner, it is desirable that the color space representation provide numerical correlates for these perceptual attributes.

The CIE system<sup>1</sup> also provides alternative color space representations that better meet the aforementioned requirements. Specifically, two alternative color space representations CIELAB and CIELUV are defined as transformations of the CIEXYZ color space both of which represent approximately uniform color spaces and provide correlates for the common perceptual attributes of *hue*, *lightness*, and *chroma*. CIELAB has been the more favored of these color space representations in the color imaging community, particularly in recent publications. The CIELAB color space representation comprises of three coordinates  $L^*$ ,  $a^*$ , and  $b^*$  defined in terms of the CIE  $X$ ,  $Y$ , and  $Z$  coordinates as

$$L^* = 116f\left(\frac{Y}{Y_n}\right) - 16, \quad (2)$$

$$a^* = 500\left(f\left(\frac{X}{X_n}\right) - f\left(\frac{Y}{Y_n}\right)\right), \quad (3)$$

$$b^* = 200\left(f\left(\frac{Y}{Y_n}\right) - f\left(\frac{Z}{Z_n}\right)\right), \quad (4)$$

where  $X_n, Y_n, Z_n$  are the tristimuli of the white stimulus, which is typically the brightest stimulus in the field of view, and  $f(\cdot) : [0, 1] \rightarrow [0, 1]$  is a 1-D function defined by<sup>‡</sup>

$$f(x) = \begin{cases} x^{\frac{1}{3}} & x > \left(\frac{6}{29}\right)^3 \\ \frac{841}{108}x + \frac{4}{29} & x \leq \left(\frac{6}{29}\right)^3 \end{cases}. \quad (5)$$

The CIELAB coordinate  $L^*$  serves as a correlate for perceived lightness/brightness and the  $a^*$  and  $b^*$  coordinates are correlates for the two opponent red-green and yellow-blue chroma axes, respectively. A hue correlate is provided by the angular position in the  $a^* - b^*$  plane

$$h_{ab}^* = \arctan\left(\frac{b^*}{a^*}\right) \quad (6)$$

and the radial distance

$$C_{ab}^* = \sqrt{(a^*)^2 + (b^*)^2}, \quad (7)$$

<sup>†</sup>We rely on the readers common intuitive understanding of these terms and refer them to the literature, for example [5, pp. 487], for more formal definitions.

<sup>‡</sup>The function  $f(\cdot)$  begins as a linear function and ends as a cube-root where the point of transition between these two functional forms is selected to ensure that the function is continuous and has a continuous first derivative everywhere, including at the point of transition.

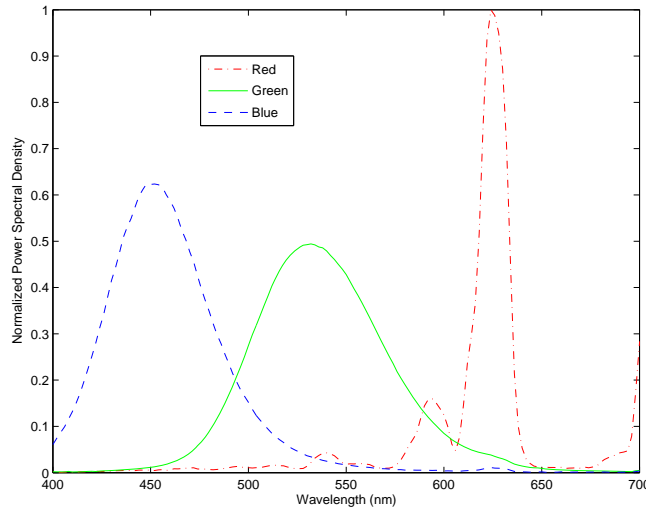


Figure 3. Normalized spectral power distributions for the primaries of a CRT Display.

in the  $a^*-b^*$  plane provides a correlate for perceived chroma.

The CIELAB color space is intended to allow computation of perceptually meaningful color differences numerically. Specifically, with respect to a standard color with CIELAB values  $L_s^*$ ,  $a_s^*$ ,  $b_s^*$ , a sample color with CIELAB values  $L^*$ ,  $a^*$ ,  $b^*$  is said to have a lightness difference  $\Delta L^* = L^* - L_s^*$ , and chroma differences  $\Delta a^* = a^* - a_s^*$ , and  $\Delta b^* = b^* - b_s^*$ , along the red-green and yellow-blue chroma axes, respectively, with the overall color difference given by the Euclidean distance

$$\Delta E_{ab}^* = \sqrt{(\Delta L^*)^2 + (\Delta a^*)^2 + (\Delta b^*)^2}. \quad (8)$$

In accordance with the design objective of a uniform color space, the Euclidean distance  $\Delta E_{ab}^*$  (delta E-ab) is intended to be perceptually uniform, i.e., if CIELAB is ideal, pairs of stimuli at the same  $\Delta E_{ab}^*$  distance from each other, are rated by observers as having the same perceptual distance between them.

### 3. THE DARK SIDE OF CIELAB: IMAGING IMPLICATIONS

In Section 1 we introduced the problems associated with the dark side of CIELAB using a physically plausible but challenging to realize visual experiment that relied on monochromatic stimuli. In this section, we highlight the impact of the dark side of CIELAB in color imaging applications, specifically in displays. Because display primaries often tend to have fairly narrow band spectra, we anticipate that the problems identified with the monochromatic stimuli in Section 1 are also inherited by the display spectra. This turns out to be indeed the case. Figure 3 illustrates the relative power spectral density measured for a cathode-ray-tube (CRT) display<sup>§</sup>. One can see that the red primary in particular is rather narrow band.

Figure 4 shows the locus of the primaries in the dark side of CIELAB by plotting the  $b^*$  vs  $a^*$  for the digital control values whose measured values are immediately adjacent to  $L^*$  values of 2.0, 1.0, and 0.5 and 0.25. One can see that although diminished by the wider spectral bandwidths, the dark side persists; large chroma values are predicted at these rather low lightness values, which are likely to be inconsistent with perception. Preliminary, psychophysical experiments conducted with the display reinforce this hypothesis.

The over-prediction of chroma for narrow-band dark stimuli in CIELAB directly impacts the utility of the space in several system design applications. In particular, our attention was drawn to the dark side of CIELAB by a display design application. Conventional display designs have optimized two-dimensional measures of gamut coverage evaluated in chromaticity space, even though the 3-D gamut determines the actual device limitations.

<sup>§</sup>Liquid crystal display (LCD) displays, particularly, those using red, green, blue light emitting diode (LED) based back-lights, encounter similar if not greater challenges. The CRT display was chosen to avoid issues of temporal and temperature stability.

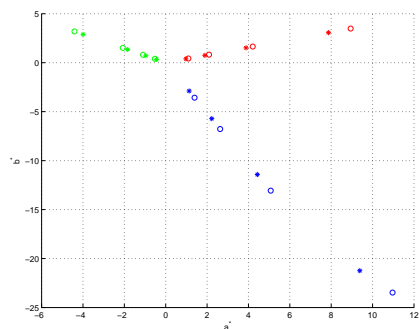


Figure 4. Measured locations of the CRT Display primaries displayed in the  $a^* - b^*$  plane at points in the immediate vicinity of  $L^*$  values of 2.0, 1.0, and 0.5 and 0.25.

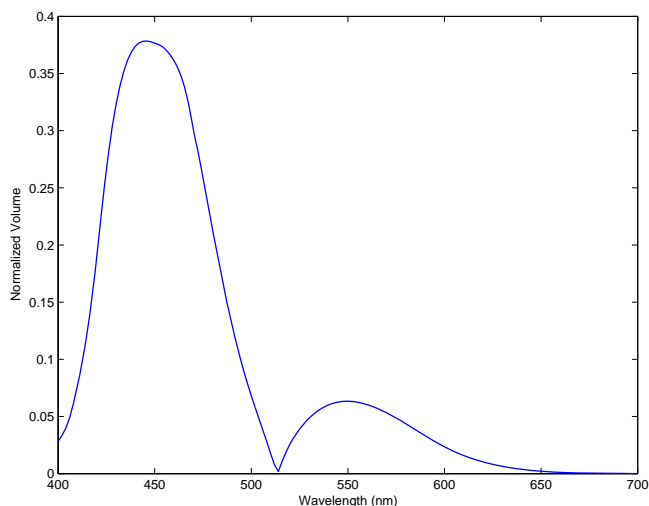


Figure 5. Normalized volume obtained by transferring one-percent of optical power from a two Red-Green primary system to a monochromatic primary, as a function of the wavelength to which power was transferred.

Motivated by these considerations, we are exploring<sup>6</sup> design methods that optimize gamut volume under other system constraints. Uniform color spaces are ideal for this setting because they offer the potential for perceptually meaningful measures of gamut volumes that mediate the appropriate trade-offs between the different dimensions of color perception. Furthermore, for mathematically well-behaved spaces the gamut volumes can also be computed efficiently, for both single and multiprimary display settings.<sup>7</sup> The problems with the dark side of CIELAB, however, severely distort the metrics making it a particularly ineffective space for this problem setting.

To appreciate the magnitude of the problem, consider a hypothetical display with the relative spectral distribution of power of two of the primaries, the red and the green, fixed to match the corresponding measured distributions shown in Fig. 3. With only two primaries, the display volume is zero. Now suppose that a small fraction, say one-percent, of the optical power is transferred from the two primaries to a third primary which is chosen to be monochromatic. As the choice of wavelength for this primary is varied over the visible range of the spectrum, the resulting volume for our system will vary. Figure 5 summarizes the results for this experiment by plotting the gamut volume in CIELAB for the three primary system obtained by transferring a rather small amount of power to the third primary against the gamut volume in CIELAB for the original three primary system, which is used as a reference here.

The plot in Fig. 5 reveals the anomaly introduced by the dark side of CIELAB for our problem setting. Even the small minuscule of power transfer considered here results in a rather large contribution to the gamut volume. The source of the problem is apparent upon looking at the gamut in CIELAB for the case corresponding to the wavelength value of 440 nm where the gamut volume for our synthesized system is close to its maximum value

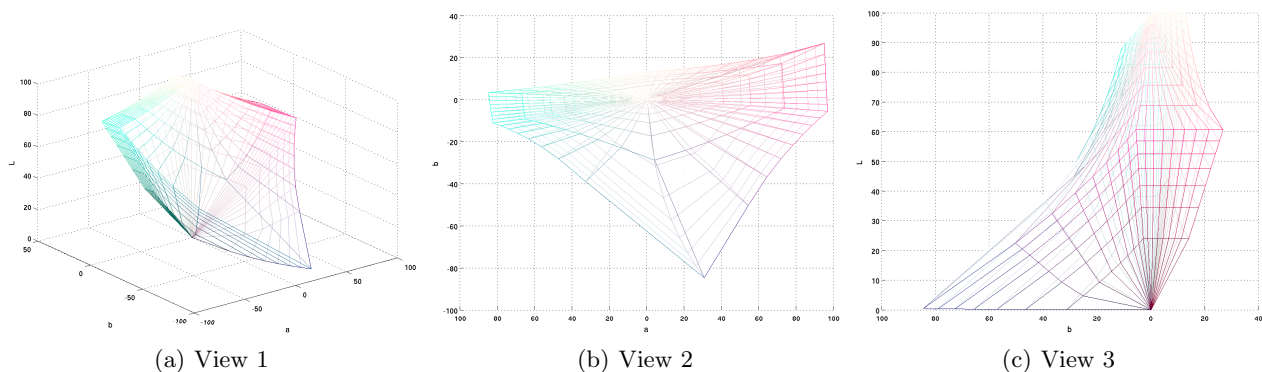


Figure 6. Three views of the CIELAB gamut obtained by taking measured red and green primaries for a CRT display and transferring one percent of the optical power to a monochromatic primary at 440 nm.

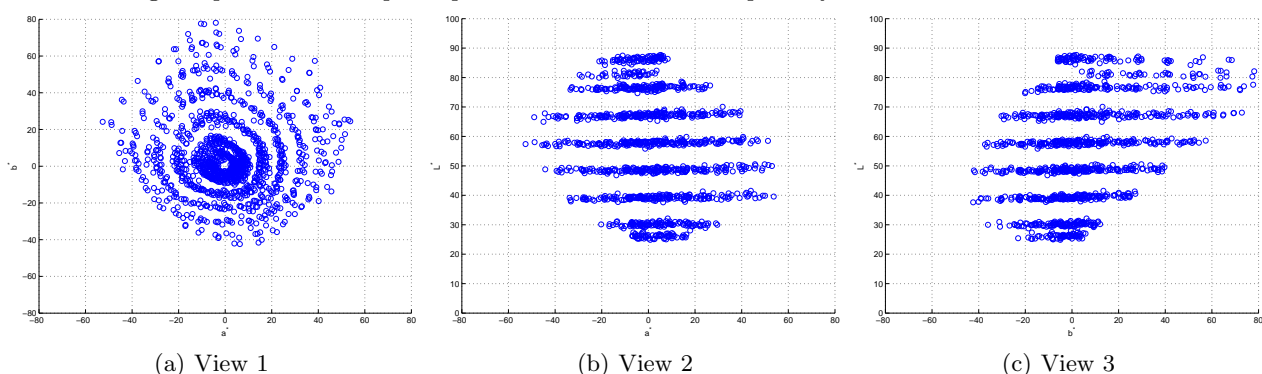


Figure 7. Location of the Munsell samples in CIELAB space.

for this experiment. Three views of the corresponding gamut in CIELAB are shown in Fig. 6. We see from the figure that the reason for the large CIELAB volume of our contrived system is the over-prediction of chroma for the primary obtained by the transfer of the rather small amount of optical power.

The relatively large impact of a low power primary on the CIELAB gamut volume, is inconsistent with visual perception and an artifact attributable to the dark side of CIELAB. When CIELAB volume is used as a design metric for display optimization, it in turn, results in artifacts, particularly in the design of multiprimary systems. This in fact is the route that brought us to this dark side.

#### 4. DISCUSSION

The problems associated with the dark side of CIELAB can be traced back to the development of the space. The Munsell color system<sup>8</sup> played a critical role in the development of the CIELAB color space<sup>¶</sup>. The Munsell system provides a system for perceptually motivated and ideally uniform notation for color along with a physical realization in the form of a color atlas of samples (to be viewed under specified illumination conditions). The Munsell system is, however, designed for surface colors viewed under daylight illumination and not for self-luminous systems. Figure 7 illustrates the locations of colors in the Munsell sample book<sup>||</sup> under CIE D65 illumination in CIELAB space. One can see that the samples do not populate the dark regions in CIELAB, in particular, there are no samples with a lightness value below a CIELAB  $L^*$  value of 24. Furthermore, at the lower lightness levels, the samples only exercise a narrow range of the chroma values.

Based on its original design CIELAB is recommended to be used for surface colors under illumination with spectral power distributions close to daylight spectra. Thus, strictly speaking, the spectrum locus region that

<sup>¶</sup>CIELAB's precursor, the ANLAB (Adams-Nickerson  $L, a, b$ ) space, made use of the Munsell system in its development.

<sup>||</sup>Based on spectrally measured data.<sup>9</sup>

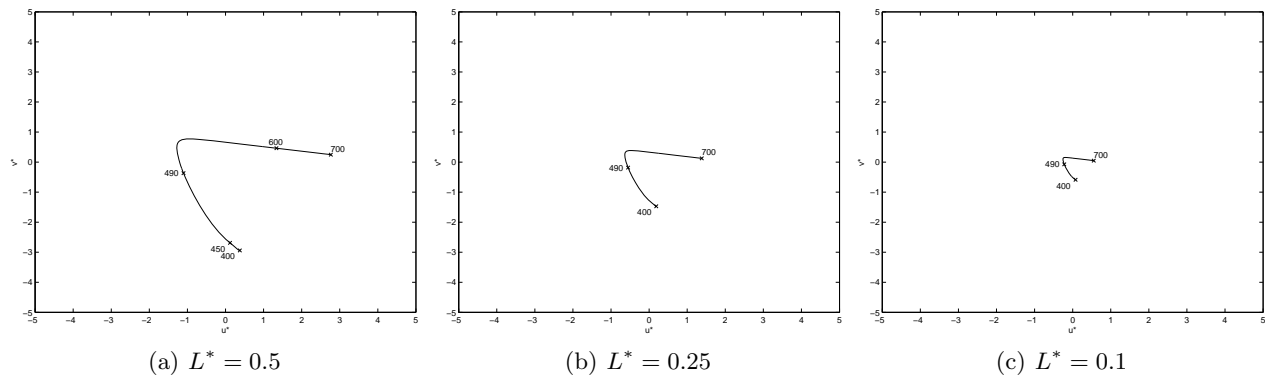


Figure 8. Paths traced by constant  $L^*$  monochromatic stimuli in the  $u^* - v^*$  plane. Sub-figures 8(a), 8(b), and 8(c) correspond to  $L^*$  values of 0.5, 0.25, and 0.1, respectively.

we explore in Fig. 2 is not intended to be domain in which CIELAB is to be used. However, in the absence of other readily alternatives, the restriction on the domain of applicability of CIELAB is often ignored in practice, motivated in part by the belief that the behavior extrapolates reasonably. The rather large deviation in the dark regions is not commonly appreciated, and the resulting problems with volume computations for display design optimization, therefore come with some surprise. The rather poor extrapolation properties of CIELAB, likely arise from the method by which the transformations in (4) and (5) were derived. The compressive nonlinear function in (5) was determined to approximate a lightness scale from luminance data. The transformation in (4) was motivated by an opponent encoding, in which the compressive nonlinearity of (5) was introduced for the normalized  $X$  and  $Z$  coordinates. The nonlinearity and the opponent encodings were introduced in terms of CIEXYZ coordinates, rather than more physiologically meaningful cone response coordinates, because the cone sensitivities of the eye were not known at the point in time that these transformations were introduced [10, pp. 67]. It is interesting to note that the functional forms chosen for transformations have a clear bearing on the extrapolation behavior. In particular, the CIELUV color space, standardized by CIE at the same time as CIELAB, does not suffer from the problems we note in the dark side of CIELAB; traces made by constant  $L^*$  monochromatic stimuli in the  $u^* - v^*$  shown in Fig. 8, show that the CIELUV representation agrees with our perceptual intuition of the range of chroma shrinking in the vicinity of the black point\*\*.

Deficiencies of CIELAB are well known in the color science community and documented in the literature. When tested on psychophysical data, the space exhibits clearly identifiable deviations from perceptual uniformity. For this reason, a number of alternative color difference formulae that utilize modified computations of color difference, instead of the simple Euclidean distance in CIELAB have also been proposed. In particular, two newer CIE standards<sup>11,12</sup> are developed in this framework. The perceptual correlates of appearance in CIELAB are also often inadequate and for this reason, newer color appearance spaces have also been recommended for use in color imaging by the CIE.<sup>13,14</sup> In part, these efforts also comprehend some of the problems that we highlight in the dark side of CIELAB. In particular, using more up to date knowledge on the cone sensitivities, the CIECAM02 color appearance space<sup>14</sup> introduces the compressive nonlinearity and the opponent encodings in terms of more meaningful physiological cone response coordinates, and in our preliminary evaluation does not immediately exhibit the problems that we note in CIELAB's dark side. These solutions, however, are not ideally suited for the system optimization type application that we outlined in Section 3. The newer color difference formulae, although significantly improved for setting color tolerances for instrumental color matching, do not provide corresponding Euclidean spaces that would allow computations of *perceptual volume*. The color appearance spaces are similarly designed with the primary objective being of enabling intuitive and perceptually meaningful manipulation of colors within a color management system and are not necessarily designed for perceptual uniformity. Equally importantly, the newer standards in both the aforementioned two categories also include a variety of transformations whose parameters are determined by regression fits to visual data, several of

\*\*The assumption that CIELAB was recommended by the CIE for reflecting samples and CIELUV for sources and displays, although a misconception [10, pp. 68], seems to find some basis in the problems observed in the dark side of CIELAB.

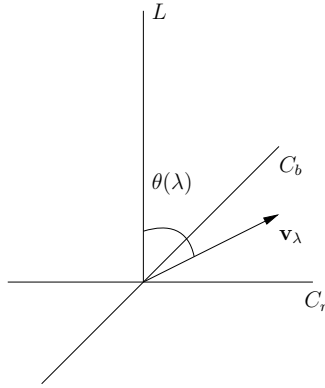


Figure 9. Illustration of the take-off angle at black for a monochromatic stimuli of wavelength  $\lambda$ .

which include higher order polynomial terms and introduce their own sources of mathematical irregularities.<sup>15–17</sup> Viewed from this perspective, color space transformations for uniform color spaces and color appearance spaces *should be evaluated not only for their agreement with recorded psychophysical data but also for their extrapolation behavior for physically feasible color regions beyond the gamut explored by the recorded data.* In several cases, fairly simple mathematical analysis can reveal some shortcomings. We illustrate this for the dark side of CIELAB next.

From our visual experience, we anticipate that at the black point, chroma cannot increase without an increase of lightness. The extent to which a color space transform  $\mathcal{F} : XYZ \rightarrow [LCrCb]$  mapping from the CIEXYZ tristimulus space to a lightness chroma  $[LCrCb]$  space agrees with this visual experience for monochromatic stimuli, can be characterized by evaluating the *take-off angle*  $\theta(\lambda)$  at the black point as a function of the wavelength  $\lambda$  of the monochromatic stimulus, defined as illustrated in Fig. 9, as the angle between the  $L^*$  axis and the vector  $\mathbf{v}_\lambda$  which represents the direction in which monochromatic stimulus with infinitesimally small power lies. If the color space transformation  $\mathcal{F}$  is mathematically well-behaved with continuous first derivatives, as is the case for CIELAB and CIELUV, then this take-off angle can be evaluated in terms of the Jacobian at the black point using a simple Taylor series analysis.

Specifically, if  $J_0$  is the Jacobian, at the black point, of the transformation from CIEXYZ tristimulus space to a lightness chroma  $[LCrCb]$ , defining

$$\mathbf{v}_\lambda = [\Delta L \ \Delta C_r \ \Delta C_b]^T = J_0[\bar{x}(\lambda) \ \bar{y}(\lambda) \ \bar{z}(\lambda)]^T,$$

we have the take-off angle

$$\theta(\lambda) = \tan^{-1} \left( \frac{\Delta L}{\Delta C} \right)$$

where  $\Delta C = \sqrt{\Delta C_r^2 + \Delta C_b^2}$ . Take off angles at black approaching 90-degrees, are inconsistent with visual experience.

Figure 10 illustrates the take-off angle at black as a function of wavelength  $\lambda$  for the CIELAB and CIELUV color spaces. For CIELAB, the rather high take-off angles, in particular, angles approaching 90-degrees for wavelengths in the region from 400 – 450 nm, highlight the problems with the dark side of CIELAB. CIELUV on the other hand behaves much better in the vicinity of black, with none of the take-off angles approaching 90-degrees. Note that, as may be anticipated based on the fact that both CIELAB and CIELUV are attempting to model the same perceptual characteristics, the pattern of variation in the take off angle shows a significant similarity for the two spaces. If the maximum perceptually acceptable take-off angle at black is characterized as a function of wavelength by psychophysical experiments, one can also test transformations fit in order to approximate perceptual color spaces, against such a characterization by using the same methodology.

For system optimization applications, there is a need for color spaces that lie between the extremes of tristimulus spaces, that are mathematically very simple but offer no perceptual uniformity or correlation with



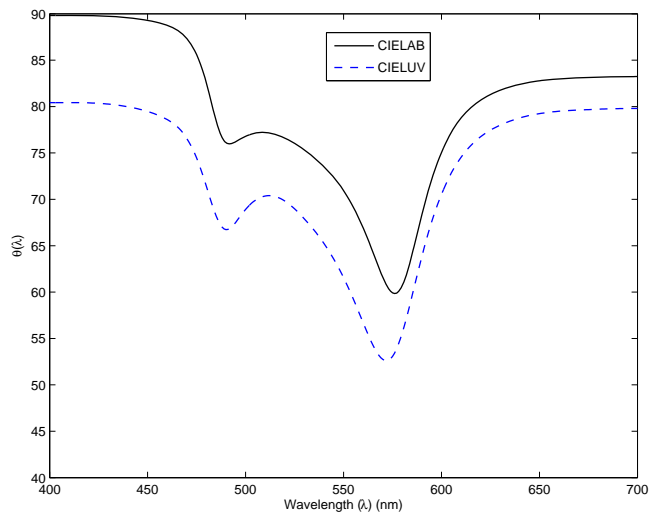


Figure 10. Take-off angle at the black point for monochromatic stimuli of different wavelengths in CIELAB and CIELUV color spaces.

appearance attributes whatsoever, and more sophisticated color spaces/difference equations that allow prediction of appearance attributes and color tolerances, but use mathematically complicated and potentially irregular transformations. For optimizing processing algorithms and system designs, it suffices if a monotone relation holds between numerical measures and perception; stronger quantitative agreement is not a crucial requirement. At the same time, because performance measures defined in terms of the approximate perceptual spaces are likely to be computed many times in the process of optimization and also for potentially for unusual choices of the parameter values, such as monochromatic stimuli, it is desirable that perceptual spaces defined for these applications be mathematically simple and extrapolate well beyond the typical gamut exercised by the psychophysical experiments. Of course, the gamut over which psychophysical data is gathered can also be expanded by using modern day color imaging devices that make it possible to conduct new experiments that can provide valuable data in regions of color space that were not explored in developing conventional standards.

## 5. CONCLUSION

An examination of the dark side of CIELAB, motivated by optimal design of display primaries, reveals not only specific shortcomings of the CIELAB space but also abundant food for thought regarding perceptual color spaces for algorithm and system optimization. Perceptual color spaces developed for these applications benefit from computational simplicity and good extrapolation behavior, auxiliary mathematical attributes that must be considered in addition to agreement with perceptual data.

## REFERENCES

- [1] CIE, "Colorimetry." CIE Publication No. 15.2, Central Bureau of the CIE, Vienna (1986). The commonly used data on color matching functions is available at the CIE web site at <http://www.cie.co.at/>.
- [2] Richards, W., "Quantifying sensory channels: generalizing colorimetry to orientation and texture, touch, and tones," *Sensory Processes* **3**(3), 207–229 (1979).
- [3] Mamlouk, A. M., Chee-Ruiter, C., Hofmann, U. G., and Bower, J. M., "Quantifying olfactory perception: mapping olfactory perception space by using multidimensional scaling and self-organizing maps," *Neuro-computing* **52**, 591–597 (2003).
- [4] Erickson, R. P., "A study of the science of taste: On the origins and influence of the core ideas," *Behavioral and brain sciences* **31**(01), 59–75 (2008).
- [5] Wyszecki, G. and Stiles, W. S., [*Color Science: Concepts and Methods, Quantitative Data and Formulae*], John Wiley & Sons, Inc., New York, second ed. (1982).

- [6] Rodríguez-Pardo, C. E. and Sharma, G., “Optimal gamut volume design for three primary and multiprimary display systems,” in [*Proc. SPIE: Color Imaging XVII: Displaying, Hardcopy, Processing, and Applications*], Eschbach, R., Marcu, G. G., and Rizzi, A., eds., **8292**, 8292–11,1–9 (Jan. 2012).
- [7] Rodríguez-Pardo, C. E., Sharma, G., Speigle, J., Feng, X., and Sezan, I., “Efficient computation of display gamut volumes in perceptual spaces,” in [*Proc. IS&T/SID Nineteenth Color and Imaging Conference: Color Science and Engineering Systems, Technologies, and Applications*], 132–138 (7–11 Nov. 2011).
- [8] Munsell, A. H., [*A Color Notation*], Munsell Color Co., Baltimore, MD, first ed. (1905).
- [9] Parkkinen, J. P. S., Hallikainen, J., and Jaaskelainen, T., “Characteristic spectra of munsell colors,” *J. Opt. Soc. Am. A* **6**(2), 318–322 (1989).
- [10] Berns, R. S., [*Billmeyer and Saltzman’s Principles of Color Technology*], Wiley-Interscience, New York, third ed. (2000).
- [11] CIE, “Industrial color difference evaluation.” CIE Publication No. 116-1995, Central Bureau of the CIE, Vienna (1995).
- [12] CIE, “Improvement to industrial colour-difference evaluation.” CIE Publication No. 142-2001, Central Bureau of the CIE, Vienna (2001).
- [13] CIE, “The CIE 1997 interim colour appearance model (simple version), CIECAM97s.” Report of the CIE Technical Committee TC1-34 (Aug. 1997).
- [14] CIE, “A colour appearance model for color management systems: CIECAM02.” CIE Technical Report 159:2004 (2004).
- [15] Sharma, G., Wu, W., and Dalal, E. N., “The CIEDE2000 color-difference formula: Implementation notes, supplementary test data, and mathematical observations,” *Color Res. Appl.* **30**, 21–30 (Feb. 2005). Paper pre-print, spreadsheet, and data available electronically at: <http://www.ece.rochester.edu/~gsharma/ciede2000/>.
- [16] Brill, M. H., “Irregularity in CIECAM02 and its avoidance,” *Color Res. Appl.* **31**(2), 142–145 (2006).
- [17] Brill, M. H. and Süssstrunk, S., “Repairing gamut problems in CIECAM02: A progress report,” *Color Res. Appl.* **33**(5), 424–426 (2008).